ACS APPLIED MATERIALS & INTERFACES

Research Article

www.acsami.org

Preparation of copper nanoparticles coated cellulose films with antibacterial properties through one-step reduction

Baoquan Jia,[†] Yan Mei,[‡] Li Cheng,[†] Jinping Zhou,[†,*] and Lina Zhang[†]

[†]Department of Chemistry, Wuhan University, Wuhan 430072, China

[‡]School of Chemistry and Chemical Engineering, Southeast University, Nanjing 210018, China

ABSTRACT: Regenerated cellulose (RC) films coated with copper (Cu) nanoparticles were prepared from cellulose-cuprammonium solution through coagulation in aq. NaOH and subsequent reduction in aq. $NaBH_4$. Structure and morphology of the nanocomposite films were characterized with X-ray diffraction (XRD), X-ray photoelectron spectroscopy (XPS), thermogravimetric analysis (TGA), scanning electron microscopy (SEM), transmission electron microscopy (TEM), and atomic force microscopy (AFM). The results established the migration of Cu^{2+} from the inner to the surface of the RC films during the coagulation of cellulose-cuprammonium solution and the reduction from Cu^{2+} to Cu^0. Cu nanoparticles were found to be firmly embedded on the surface of the RC films. The RC films coated with Cu nanoparticles showed efficient antibacterial activity against *Staphylococcus aureus* (*S. aureus*) and *Escherichia coli* (*E. coli*). The dramatic reduction of viable bacteria could be observed within 0.5 h of exposure, and all of the bacteria were killed within 1 h.

KEYWORDS: *copper nanoparticles, cellulose, nanocomposite film, one-step reduction, antibacterial*

1. INTRODUCTION

Cellulose is one of the most common organic polymers that is considered as an almost inexhaustible source of raw material for the increasing demand for making environmentally friendly and biocompatible products.[1,2] Cellulose products are widely used in the fields of textiles, packaging, medical supplies, etc. Besides as a conventional material, cellulose products are also present in the field of electronic device,[3] biomedical materials,[4] and energy storage.[5] Usually, these cellulose materials have no antibacterial activity, and sometimes may promote further growth of microorganisms. Especially, those products that human are often exposed to, will carry bacteria and therefore, cause disease. Hence, the antibacterial activity induced cellulose products are expected to promote their safe use. Recent outbreaks caused by bacteria make antibacterial study more urgent, and many researchers have conducted studies to modify the cellulose products. The antibacterial activity can be usually achieved through modifying surface,[6,7] blending bactericides,[8] loading silver nanoparticles,[9,10] etc. Improving the antibacterial performance of cellulose materials using facile approaches intrigues many researchers.

It is known that copper (Cu) is a broad-spectrum biocide and effectively inhibits the growth of bacteria, fungi and algae.[11] Recent works reported that Cu at nanoscale forms exhibits good antibacterial activity,[12,13] and the products with Cu-containing surfaces may meet hospital requirements.[14] Different from silver (Ag) which has been studied extensively for antibacterial application, Cu is an essential element for living organisms, and it might even be suitable for biomedical applications. Moreover, Cu is currently cheaper than Ag in the market and therefore, a method utilizing Cu would proves to be quite cost-effective. The general mechanism of antibacterial activity of nanoscale metal-based material (Ag, Cu, etc.) is still uncertain. Some studies proposed that enhanced metal-ion release and specific interaction between the organism and nanomaterial played a role in the antibacterial process.[15−17] In addition to the antibacterial performance, Cu is also useful in energy, information technology and catalysis.[18]

Aqueous cuprammonium hydroxide is a suitable solvent for polysaccharides, polyglucans, proteins, and so on. The cuprammonium process is used to produce regenerated cellulose (RC) materials, such as film, fiber and nonwoven cloth. During the production of RC films from cellulose-cuprammonium solution, the Cu^{2+} was removed by H_2SO_4 treatment after coagulation in aq. NaOH.[19] Moreover, the Cu compounds removed by acid need to be recovered. Contrastingly, instead of being removed by acid, in this study, the Cu compound will be utilized to fabricate RC films coated with Cu nanoparticles. Strickland et al.[13] prepared Cu nanoparticles coated fibrous cellulose substrates, showing more efficient antibacterial activity and better biocompatibility than those coated with Ag nanoparticles. Ag nanoparticles coated cellulose substrates are promising in the application of wound-dressing materials. Ordinary methods of coating nanoparticles require depositing nanoparticles externally, and the particles are not firmly fixed. This may be resolved by mechanically fixing the nanoparticles on the surface of cellulose matrix. This study aims at improving the antibacterial activity of cellulose films by embedding Cu nanoparticles on the surface of the RC film by using copper compounds of cellulose-cuprammonium solution. The structure, morphology and antibacterial properties of the films were investigated.

2. EXPERIMENTAL SECTION

2.1. Materials. Cotton linter pulp was provided by Hubei Chemical Fiber Group Ltd. (Xiangfan, China). $CuSO_4 \bullet 5H_2O$,

Received: January 1, 2012
Accepted: June 8, 2012
Published: June 8, 2012

   dx.doi.org/10.1021/am3007609 | *ACS Appl. Mater. Interfaces* 2012, 4, 2897−2902

Scheme 1. Schematic presentation of the preparation of cellulose film containing Cu compounds (F0), RC film (F1) and Cu/cellulose nanocomposite (F2)

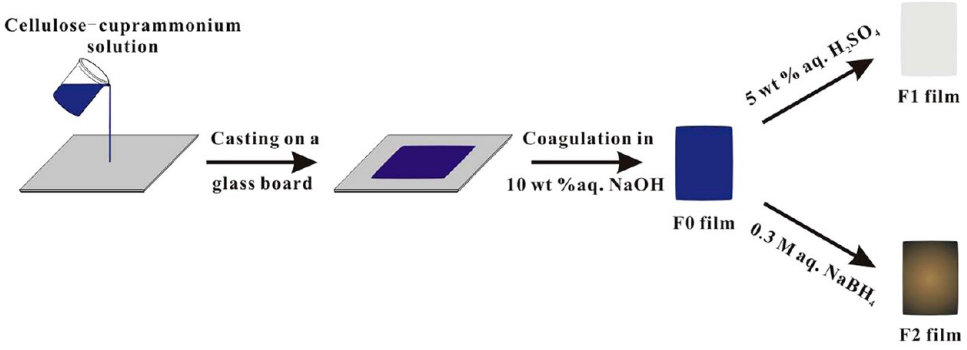

NaOH, and ammonia solution were of analytical grade and $NaBH_4$ (96%) were purchased from Sinopharm Chemical Reagent Co., Ltd. (Shanghai, China), and used without further purification. The types of bacteria are ATCC.

2.2. Preparation of the regenerated cellulose and nanocomposite film. Cotton linter was dissolved in aqueous cuprammonium hydroxide according to the known process with the cellulose concentration of 8 wt %,[18] and the blue viscous solution was obtained. The molar composition of Cu/NH_3 in solution was adjusted at 0.046/0.36. As shown in Scheme 1, the cellulose-cuprammonium solution was cast on a glass board and subsequently coagulated in 10 wt % NaOH aqueous solution for 10 min. The blue films were then transferred to a distilled water bath to remove NaOH and ammonium. The films as-obtained were coded as F0. Some F0 films were treated with 5 wt % H_2SO_4 aqueous solution to dissolve the copper compounds and then washed with distilled water and these pure RC films were coded as F1. The other F0 films were placed in 0.3 M $NaBH_4$ aqueous solution at 5 °C for 5 h and then washed with distilled water, and the obtained Cu/cellulose nanocomposite films were coded as F2. All the films were air-dried after treatments.

2.3. Characterization. X-ray diffraction (XRD) measurements were carried out on an XRD diffractonmeter (D8-Advance, Bruker, Germany). The patterns with Cu Kα radiation (λ = 0.15418 nm) at 40 kV and 30 mA were recorded in the 2θ region from 10 to 80° for the films maintaining a scanning speed of 4°/min. X-ray photoelectron spectra (XPS) were recorded on a Kratos XSAM800 X-ray photoelectron spectrometer, using Mg Kα radiation as the excitation source. Thermogravimetric analysis (TGA) was applied on a NETZSCH STA449c/3/G thermal analyzer (NETZSCH, Germany). The primary thermograms were recorded in the temperature range of ambient to 800 °C at a heating rate of 10 °C/min under an air atmosphere.

Transmission electron microscopy (TEM) was performed on a JEM 2010 FEF (UHR) microscope (JEOL, Japan) at 200 kV. The F0 and F2 films were embedded in epoxy resin, ultrathin slices for TEM measurements were obtained by sectioning on an LKB-8800 ultratome. Scanning electron microscopy (SEM) images were taken on QUANTA scanning electron microscope (FEI Co., Netherlands). The samples were sputtered with gold for SEM measurement. Atomic force microscopy (AFM) was used to examine the surface morphology on a scanning probe microscope (SPM-9500J3, Shimadzu, Japan).

Water contact angle was measured on a drop shape analysis system (DSA100, KRÜSS, Germany). Before measurement of water contact angle, F2 film was photochemically cleaned by UV/ozone cleaning at a nitrogen atmosphere for 5 min to remove the organic contaminants on the surface. The source of light employed was an exciter lamp with λ = 172 nm (10 mW cm^{-2}, Ushio Electric, UER20−172V, Japan).

2.4. Testing of antibacterial activity. The antibacterial activity of the films was tested against Gram-positive bacteria *S. aureus* and Gram-negative bacteria *E. coli*. The suspension of bacteria cells had a final density of 10^6 cells/mL in PBS solution. The F1 and F2 films (1 cm ×1 cm) were first washed with 75% ethanol to kill bacteria, and then immersed in 5 mL of the bacterial suspension in an Erlenmeyer flask and the solution was shaken at 200 rpm at 37 °C. The viable cell counts of bacteria were measured by surface spread plate method. Specifically, after 0, 0.5, 1, and 2 h, 0.2 mL of bacterial culture were taken from the flask and serial dilutions with PBS were repeated with each initial sample, respectively. 0.1 mL diluent of the sample was then spread onto solid growth agar plates. After incubation of the plates at 37 °C for 24 h, the number of viable cells was counted manually and multiplied by the dilution factor.

3. RESULTS AND DISCUSSION

3.1. Fabrication of Cu nanoparticles coated cellulose film. Scheme 1 illustrates the preparation of the regenerated

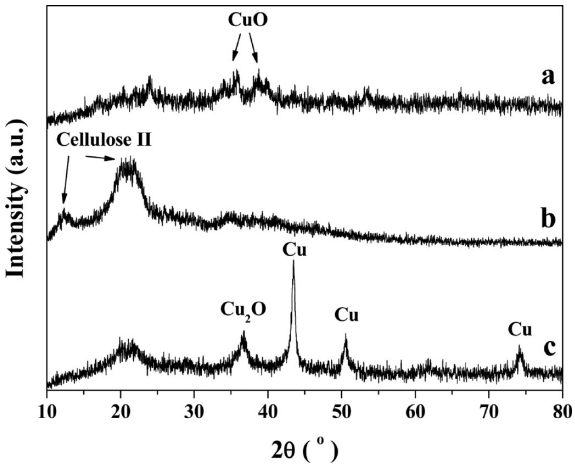

Figure 1. XRD patterns of (a) F0 film, (b) F1 film and (c) F2 film.

cellulose films coated with Cu nanoparticles. After casting the cellulose-cuprammonium, the glass board was immersed in aq. NaOH bath. During coagulation in aq. NaOH, the cuprammonium complex was dissociated. The XRD peaks corresponding to CuO were observed due to the loss of water after drying the F0 film (Figure 1a). The RC film (F1) was prepared by immersing the F0 film into an acid solution for acid etch. As illustrated in Figure 1b, the peaks at 2θ = 12, 20, and 22° were assigned to the ($\bar{1}$10), (110), and (200) planes of cellulose II crystalline form.[21] For F2 film, aq. $NaBH_4$ was used to reduce Cu^{2+} inside the film (Figure 1c). The presence of Cu_2O was observed probably because the incomplete reduction in the interior film. When we increased the concentration of $NaBH_4$ to 0.4 M, the Cu_2O peak became weaker. Moreover, the metallic copper, present after initial reduction, underwent air oxidation to copper oxide, hence, likely leaving Cu/Cu_2O and

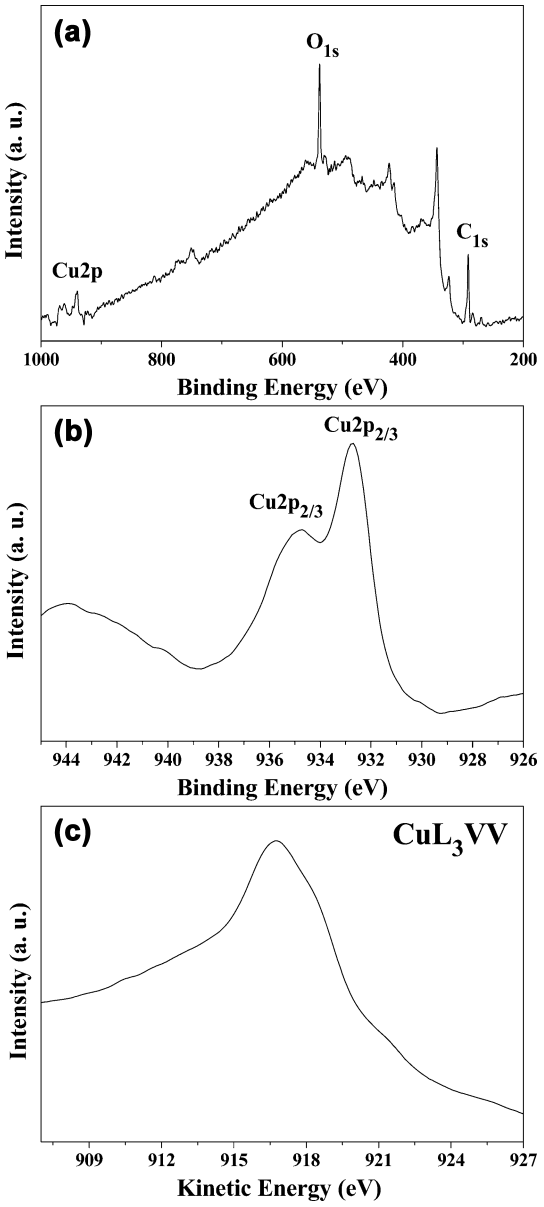

Figure 2. XPS (a and b) and Auger (c) spectra of the surface of F2 film.

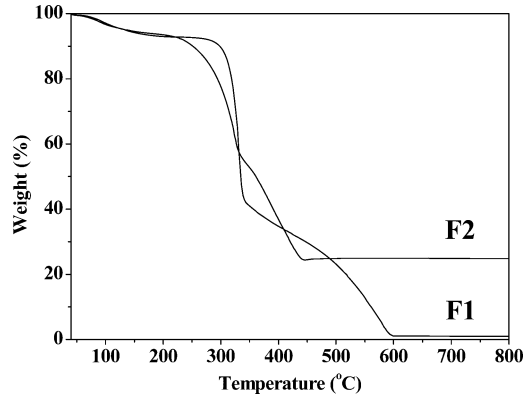

Figure 3. Primary thermograms of F1 and F2 films under an air atmosphere.

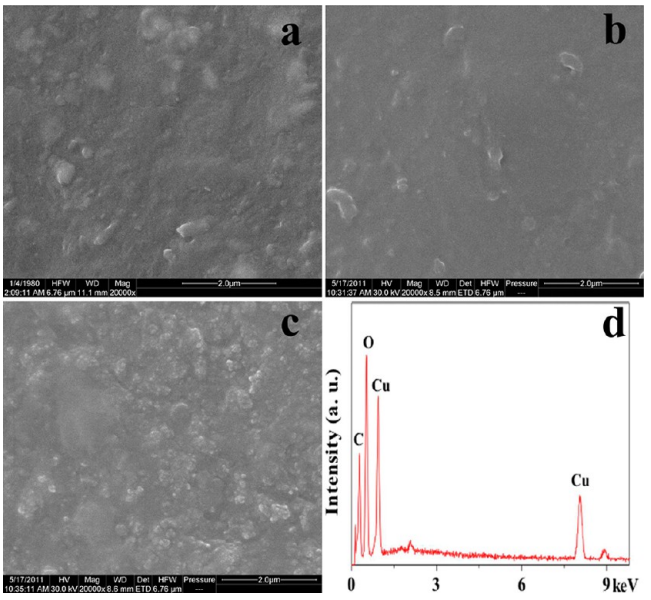

Figure 4. SEM images of the surface of (a) F0, (b) F1 and (c) F2 films. (d) EDS spectrum of F2 film.

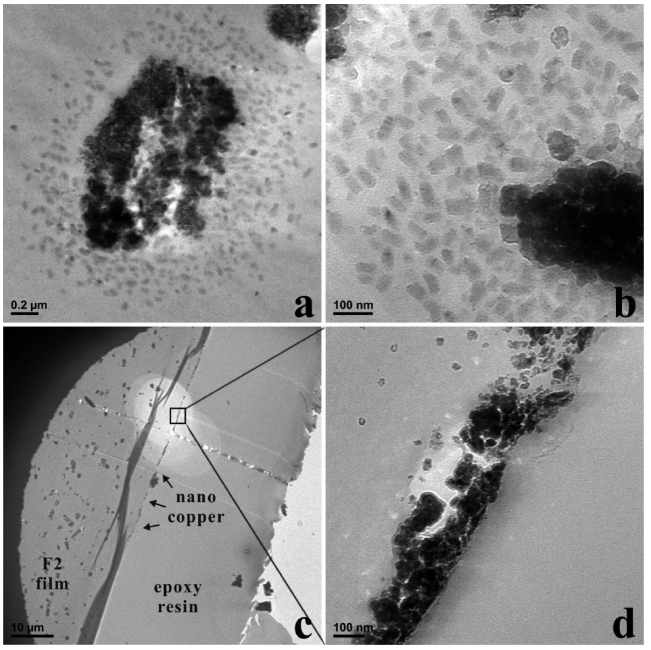

Figure 5. TEM images of the ultrathin cross-section slices of (a and b) F0 and (c and d) F2 films.

$Cu/Cu_2O/CuO$ nanocomposites. The XPS analysis was further carried out to examine the chemical composition on the surface of F2 film. Signals for Cu $2p_{2/3}$ were detected in Figure 2a indicating the deposition of Cu on the surface due to the investigation depth of XPS. The signals could be fit with two components (Figure 2b), centered at 932.6 and 934.7 eV. The two peaks were consistent with Cu^0 or Cu^+ (Cu_2O), and Cu^{2+} (CuO), respectively.[22,23] The corresponding Cu(L_3VV) Auger spectrum in Figure 2c shows the peak at 916.8 eV attributing to Cu^+.[23] It indicated the presence of Cu_2O at the outermost layer. The presence of copper oxides was the result of the complex process of reduction of Cu^{2+} by $NaBH_4$; the experimental conditions have great influence over the reaction product.[24] At the same time, the surface of metallic copper in the nanosize

dx.doi.org/10.1021/am3007609 | ACS Appl. Mater. Interfaces 2012, 4, 2897−2902

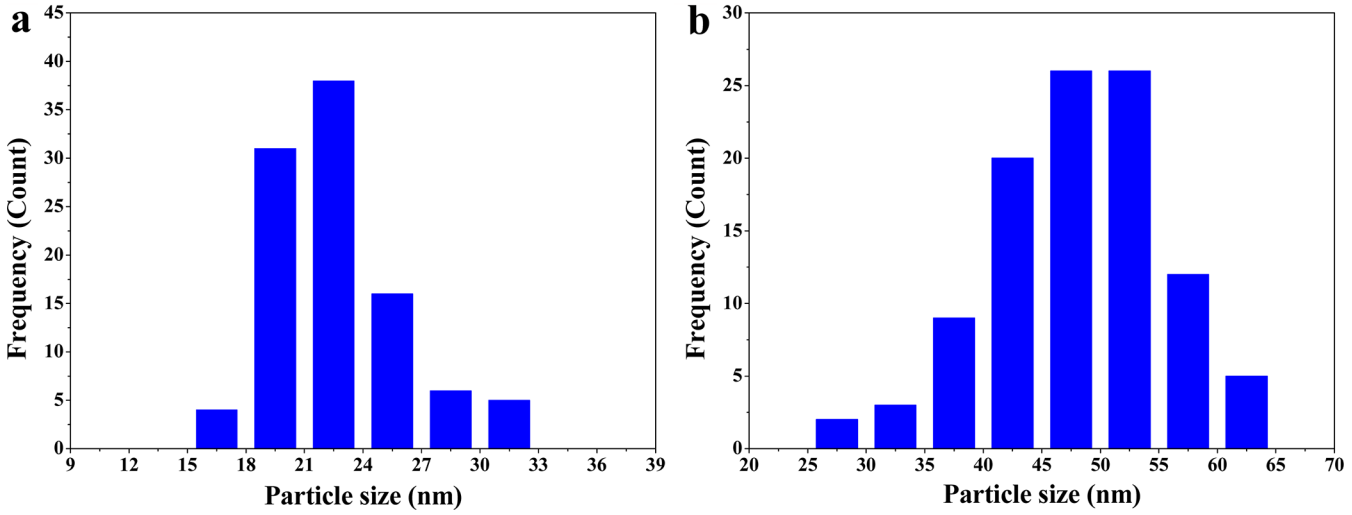

Figure 6. Size distribution of Cu nanoparticles (a) in the film and (b) on the surface of the film. Histogram (a) was measured by TEM image (22.5 ± 3.5 nm), and (b) was measured by SEM image(47.5 ± 8.5 nm).

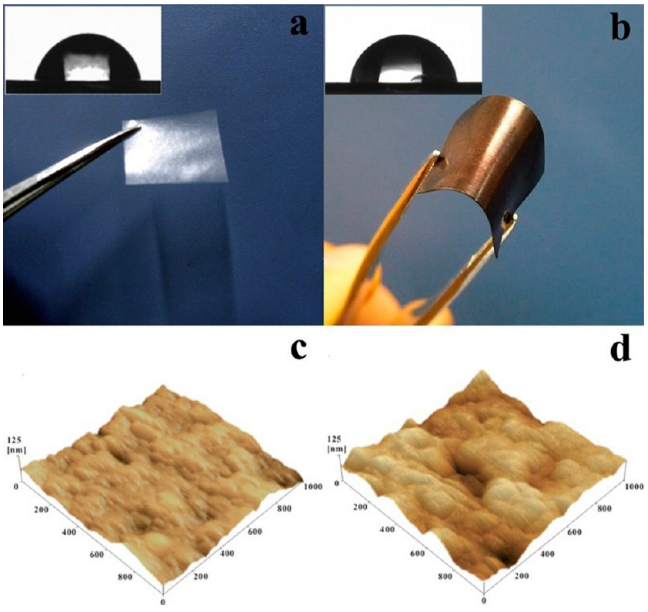

Figure 7. Photographs and water contact angles of (a) RC film (F1) and (b) Cu nanoparticles coated RC film (F2). AFM 3D images of the surface of (c) F1 and (d) F2 film. (Area: 1000 nm ×1000 nm, z: 0 - 125 nm).

regime was not very stable. It had been reported that the nanosized metallic copper using borohydride reduction showed facile oxidation upon the presence of air.[25] Oxidation was very probable to happen for our samples as the drying and storage of the samples were exposed to air without any antioxidant treatment or protection.

Figure 3 displays the thermogravimetric curves of F1 and F2 films under an air atmosphere. A small weight loss observed in 80−120 °C range was related to the release of moisture from the samples. The pure RC film (F1) showed a two-step thermal degradation process with elevating temperature. The first obvious weight loss was found in the temperature range 300−350 °C, which was attributed to the onset of cellulose decomposition. The second weight loss peak of RC at 400−530 °C was caused by oxidation and burning of cellulose. Thermal stability of the F2 film apparently decreased owing to the catalytic property of Cu nanoparticles. Especially, the second weight loss stage of the F2 film was shifted to the temperature lower than 430 °C. According to the amount of residues, the content of Cu nanoparticles in the F2 film was estimated to be 21 wt % by TGA measurement.

3.2. Morphology of the Cu nanoparticles coated film.

Figure 4 shows the SEM images of the films under study. The differences in the surface of the F0, F1 and F2 films were clearly illustrated. The original film (F0) and acid-treated film (F1) displayed a relatively flat surface with some uneven regions, which could be owing to the open and simple casting process employed. However, the regenerated cellulose film coated with Cu nanoparticles (F2) exhibited a rough surface (Figure 4c). Large numbers of particles were embedded on the surface of RC films. The micrographs illustrate that the Cu^{2+} inside the film migrated to the surface during the reduction with $NaBH_4$. It was because of the different concentrations of $NaBH_4$ inside and outside the film. After it was air-dried, the swollen film turned into a denser structure, leading to a firm fixation of nanoparticles on the surface of the film. The particles were not evenly dispersed on the surface, where aggregation could be observed according to Figure 4c. The energy dispersive spectrum (EDS) from SEM indicated that there were O, C and Cu elements in the composite film.

Figure 5a and 5b show the micro presentation of F0 film ultrathin slices. From these micrographs, it is evident that the nanoparticles were dispersed in the cross-section of RC matrix unevenly and many of them were aggregated closely. The rapid coagulation might account for the uneven dispersion of nanoparticles inside the films. Further, the regions around the aggregates indicate the presence of rod like free particles with about 60 nm length and 25 nm diameter. The formation of this nanorod during the process of coagulation in NaOH was not clear, however, it might have occurred due to the interaction between cuprammonium and cellulose macromolecules and the inner porous structure of the cellulose film. The F2 film was also embedded in epoxy resin and ultrathin slices were sectioned. In Figure 5c and 5d, TEM images of the F2 film which was the result of F1 film reduced by aq. $NaBH_4$ are displayed. After reduction in aq. $NaBH_4$, the shape of particles became irregular and many particles near the edge migrated to the surface of the film. A distinct line made of Cu nanoparticles

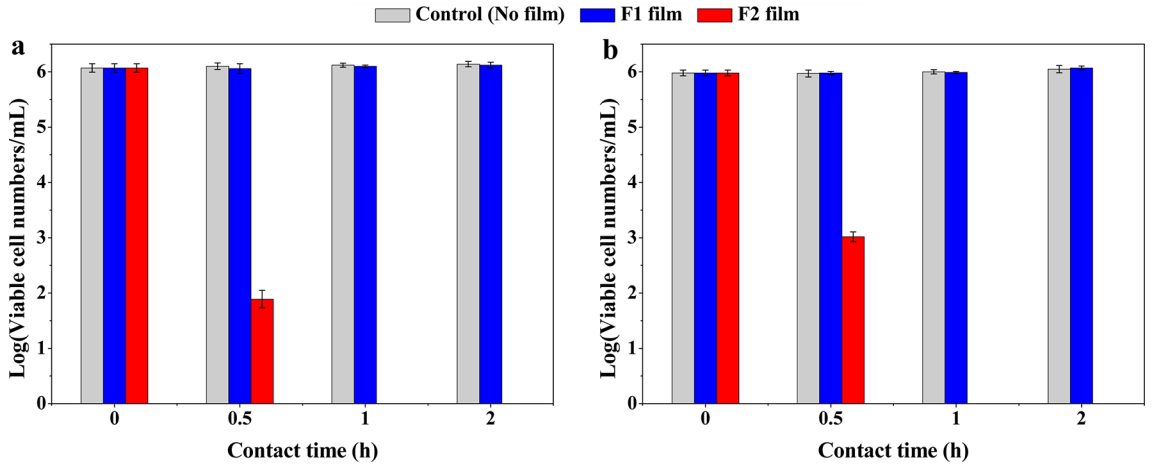

Figure 8. Viable cell numbers of (a) *S. aureus* and (b) *E. coli* on the control group, RC film (F1) and Cu nanoparticles coated RC film (F2) with contact time.

could be seen, which corresponded to the particles on the surface (Figure 5c). On the left of the line was the F2 film and on the right was the epoxy resin according to the dispersion of particles. In the micrograph, aggregates of Cu nanoparticles dispersed inside the film can be observed on the left of the line. However, in the area near the Cu line, there were fewer aggregates than in the inner part and the surface of the film. It suggests that the particles that had been originally in the blank zone moved. This unequivocally indicates the migration of Cu^{2+} during the coagulation and reducing processes. Figure 5d displays an enlarged view of the marked region, and illustrates the collection of Cu nanoparticles on the surface of the F2 film. The dispersion of the particles showed the tendency of the collection toward the line. The size and number of the particles increased on approaching the surface of the F2 film.

The size of particles inside and on the surface of the film was measured using TEM and SEM images, respectively. For this purpose, 100 particles in these images were considered. The mean size of particles inside the film (Figure 5d) was 22.5 nm, with a standard deviation of 3.5 nm. Similarly, the mean size of the particles on the surface as measured by SEM (Figure 4c) was 47.5 nm with a standard deviation of 8.5 nm. This clearly indicates that the size of the particles increased on approaching the surface of the F2 film. The histograms of size distribution are shown in Figure.6. The difference in particle size and size distribution between the particles inside and outside indicated that the particles on the surface aggregated during the reduction by $NaBH_4$. Furthermore, it also supported the migration process.

3.3. Wettability of nano Cu coated cellulose film. The digital photographs of F1 and F2 films are shown in Figure 7a and b, respectively. In contrast to the transparent RC films (F1), the nanocomposite films (F2) were bronze-colored. It had been reported that Cu nanoparticle was used to fabricate a superhydrophobic surface and the water contact angle was above 160°.[26] AFM was carried out to investigate the roughness and surface topography of F1 and F2 films (as shown in Figure 7c and 7d). The F2 film surface was noticeably rougher than F1 film. The arithmetic mean roughness (Ra) and square average roughness (Rms) for the surface of F1 film were 9.31 and 11.87 nm, respectively. Ra and Rms of the surface of F2 film were 17.20 and 20.86 nm, respectively. It suggests that the surface roughness of F2 film was greater than F1 film. The wettability was examined to investigate the influence of Cu nanopartiles over the wetting property of the film surface. The water contact angle of RC film was 77.5 ± 2.6° (Figure 7a), indicating a typical hydrophilic surface. The water contact angle of the RC coated with Cu nanoparticles was 110 ± 0.4° before UV-ozone cleaning. However, after 5 min cleaning by UV-ozone, the water contact angle dropped to 81.1 ± 1.8° (Figure 7b), which was very close to that of RC film. Owing to the adsorption of moisture and organic contaminants at laboratory environment, the reduction of surface energy could occur for many materials.[27] White[28] proposed that vapor of mineral oil could adsorb on transition metals, and organics could be gathered from the air by adsorption onto oxidized metal surfaces. Thus, in this work, Cu nanoparticles alone did not change the wettability of the composite film actually.

3.4. Antibacterial properties. To evaluate the antibacterial activity of the F2 film, the surface spread plate method was utilized. *S. aureus* and *E. coli* were chosen to assess the varying performances of F1 and F2 films. As shown in Figure 8, the results of the tests show distinct differences between the two kinds of films for antibacterial activity. As currently envisioned, RC films had no antibacterial activity in the tests. *S. aureus* and *E. coli* on the surface of the RC film were not killed, and the number of viable bacteria remained static as they were initially. However, within 0.5 h exposure, 4-log reduction and 3-log reduction in viable bacteria of *S. aureus* and *E. coli* were observed, respectively, when using the Cu/cellulose nanocomposite film. Further, after 1 h of exposure, both these bacteria were annihilated by F2 film. At the surface of composite film, where the interaction between bacteria and film happened, it was embedded with Cu nanoparticles. Cu is one kind of long lasting biocide as the release of Cu is very slow and in small quantities.[29] The nanocomposite film showed rapid sterilization to both *S. aureus* and *E. coli*, which should be due to the release of Cu ions into culturing medium. Since chloride ions in PBS solution would significantly reduce the concentration of Cu ions, the interaction between Cu nanoparticles and microorganism played an important role in the antibacterial activity.[13,16] The results suggest that the regenerated cellulose films coated with Cu nanoparticles can be considered as potential materials as biocide in medical and related fields.

dx.doi.org/10.1021/am3007609 | *ACS Appl. Mater. Interfaces* 2012, 4, 2897−2902

4. CONCLUSIONS

In summary, through the one-step reduction in aq. $NaBH_4$, Cu nanoparticles coated cellulose films were prepared. Different from the ordinary deposition from the outside, we made use of the copper compounds that were derived from cuprammonium process and left inside the film after coagulation. Through reduction in aq. $NaBH_4$, Cu nanoparticles were embedded on the surface of the film and fixed by the cellulose matrix. There was a migration of Cu^{2+} to the surface during the coagulation and reduction processes attributed to the concentration difference inside and outside the film. However, although the surface morphology was altered by Cu nanoparticles, the surface energy had no significant change. The wetting properties were the same for RC film and nanocomposite film. The nanocomposite film exhibited a strong and efficient antibacterial activity against *S. aureus* and *E. coli*. All the bacteria were killed within 1 h, and the dramatic reduction of viable bacteria could be observed within 0.5 h. The rapid killing effect was not only because of the release of Cu ions, but the contact-killing also played an important role. These characteristics increase the scope of applications of the Cu/cellulose nanocomposite film in biomedical, catalysis, packaging, and electronics.

AUTHOR INFORMATION

Corresponding Author

*Corresponding author. Tel.: +86 27 87219274. Fax: +86 27 68754067, E-mail address: zhoujp325@whu.edu.cn (J. Zhou).

Notes

The authors declare no competing financial interest.

ACKNOWLEDGMENTS

This work is supported by the National Natural Science Foundation of China (50973085), Program for New Century Excellent Talents in University (NCET-11-0415) and the National Basic Research Program of China (973 Program, 2010CB732203). We acknowledge the Center for Electron Microscope of Wuhan University for the technical support.

REFERENCES

(1) Klemm, D.; Heubletin, B.; Fink, H.-P.; Bohn, A. *Angew. Chem., Int. Ed.* **2005**, *44*, 3358−3393.
(2) Klemm, D.; Kramer, F.; Moritz, S.; Lindström, T.; Ankerfors, M.; Gray, D.; Dorris, A. *Angew. Chem., Int. Ed.* **2011**, *50*, 5438−5466.
(3) Yun, S.; Jang, S. D.; Yun, G. Y.; Kim, J. H.; Kim, J. *Appl. Phys. Lett.* **2009**, *95*, 104102.
(4) Tsioptsias, C.; Panayiotou, C. *Carbohydr. Polym.* **2008**, *74*, 99−105.
(5) Weng, Z.; Su, Y.; Wang, D. W.; Li, F.; Du, J. H.; Cheng, H. M. *Adv. Energ. Mater.* **2011**, *1*, 917−922.
(6) Zemljič, L. F.; Peršin, Z.; Stenius, P. *Biomacromolecules* **2009**, *10*, 1181−1187.
(7) Chen, S.; Chen, S.; Jiang, S.; Xiong, M.; Luo, J.; Tang, J.; Ge, Z. *ACS Appl. Mater. Interfaces* **2011**, *3*, 1154−1162.
(8) Shih, C. M.; Shieh, Y. T.; Twu, Y. K. *Carbohydr. Polym.* **2009**, *78*, 169−174.
(9) Tankhiwale, R.; Bajpai, S. K. *Colloid. Surface B: Biointerfaces* **2009**, *69*, 164−168.
(10) Sureshkumar, M.; Siswanto, D. Y.; Lee, C. K. *J. Mater. Chem.* **2010**, *20*, 6948−6955.
(11) Dollwet, H. H. A.; Sorenson, J. R. *J. Trace Elem. Med. Bio.* **1985**, *2*, 80−87.
(12) Raffi, M.; Mehrwan, S.; Bhatti, T. M.; Akhter, J. I.; Hameed, A.; Yawar, W.; ul Hasan, M. M. *Ann. Microbiol.* **2010**, *60*, 75−80.
(13) Cady, N. C.; Behnke, J. L.; Strickland, A. D. *Adv. Funct. Mater.* **2011**, *21*, 2506−2514.
(14) Mikolay, A.; Huggett, S.; Tikana, L.; Grass, G.; Braun, J.; Nies, D. H. *Appl. Microbial. Biot.* **2010**, *87*, 1875−1879.
(15) Sondi, I.; Salopek-Sondi, B. *J. Colloid Interface Sci.* **2004**, *275*, 177−182.
(16) Hwang, E. T.; Lee, J. H.; Chae, Y. J.; Kim, Y. S.; Kim, B. C.; Sang, B. I.; Gu, M. B. *Small* **2008**, *4*, 746−750.
(17) Pang, H.; Gao, F.; Lu, Q. *Chem. Commun.* **2009**, 1076−1078.
(18) Gao, F.; Pang, H.; Xu, S.; Lu, Q. *Chem. Commun.* **2009**, 3571−3573.
(19) Yang, G.; Yamane, C.; Matsui, T.; Miyamoto, I.; Zhang, L.; Okajima, K. *Polym. J.* **1997**, *29*, 316−332.
(20) Miyamoto, I.; Inamoto, M.; Matsui, T.; Saito, M.; Okajima, K. *Polym. J.* **1995**, *27*, 1113−1122.
(21) Kaplan, D. L. In *Biopolymers from Renewable Resources*; Abe, A., Monnerie, L., Shibaev, V., Suter, U. W., Tirrell, D., Ward, I. M., Eds.; Spinger-Verlag: Berlin Heidelberg, 1998; p 55.
(22) Lei, J.; Rudenja, S.; Magtoto, N.; Kelber, J. A. *Thin Solid Films* **2006**, *497*, 121−129.
(23) Strohmeier, B. R.; Levden, D. E.; Field, R. S.; Hercules, D. M. *J. Catal.* **1985**, *94*, 514−530.
(24) Shen, J.; Li, Z.; Yan, Q.; Chen, Y. *J. Phys. Chem.* **1993**, *97*, 8504−8511.
(25) Sinha, A.; Das, S. K.; Kumar, T. V. V; Rao, V.; Ramachandrarao, P. *J. Mater. Synth. Process* **1999**, *7*, 373−377.
(26) Shirtcliffe, N. J.; McHale, G.; Newton, M. I.; Perry, C. C. *Langmuir* **2005**, *21*, 937−943.
(27) Drelich, J.; Chibowski, E.; Meng, D. D.; Terpilowski, K. *Soft Matter* **2011**, *7*, 9804−9828.
(28) White, M. L. In *Clean Surfaces: Their Preparation and Characterization for Interfacial Studies*; Goldfinder, G., Eds.; Marcel Dekker: New York, 1970; p 361−367.
(29) Drelich, J.; Li, B.; Bowen, P.; Hwang, J. Y.; Mill, O.; Hoffman, D. *Appl. Surf. Sci.* **2011**, *257*, 9435−9443.